Journal of

Applied and Computational Mechanics

Shahid Chamran
University of Ahvaz

Research Paper

Magnetic Field Influence on Thermophoretic Micropolar Fluid Flow over an Inclined Permeable Surface: A Numerical Study

Parakapali Roja[1], Thummala Sankar Reddy[2], Shaik Mohammed Ibrahim[3], Meruva Parvathi[1], Gurram Dharmaiah[4], Giulio Lorenzini[5]

[1] Department of Mathematics, Annamacharya Institute of Technology and sciences, Rajmpeta, Kadapa-516126, A.P., India

[2] Department of Mathematics, Annamacharya Institute of Technology and sciences, C. K. Dinne, Kadapa-516003, A.P., India

[3] Department of Engineering Mathematics, College of Engineering, Koneru Lakshmaiah Education Foundation, Vaddeswaram, Andhra Pradesh – 522302, India

[4] Department of Mathematics, Narasaraopeta Engineering College, Narasaraopet, 522601, Andhra Pradesh, India

[5] Department of Engineering and Architecture, University of Parma, Parco Area delle Scienze 181/A, Parma 43124, Italy

Abstract. The researchers have reported numerous numerical and analytical efforts in recent years to understand technological and industrial processes. Microelectronics, heat exchangers, solar systems, energy generators are just a few numbers of recent applications of heat and mass transfer flow. Two dimensional steady incompressible MHD flow of micropolar fluid over an inclined permeable surface with natural convection is investigated in this research work, with the contribution of thermal radiation under thermophoretic effects as a heating source. As a result of this infestation, mathematical model of the problem equations based on energy, momentum, angular momentum, mass, and concentration are developed. To convert the current problem into dimensionless ordinary differential equations, non-dimensional variables have been assigned. The evolved mathematical model is numerically solved aside utilizing Shooting technique along with 4th order R-K method solver in MATHEMATICA. The outcomes are displayed and analyzed through figures and tables. Finally, skin friction, Nusselt and Sherwood numbers are tabulated for distinct parameter-factors. To validate the accuracy of numerical method used in this problem, we compare the numerical results with available findings, and it is evident that the outcomes of current work are in good agreement with those reported in the literature. Improving the values of thermophoresis, radiation factors, and Schmidt number, declines the velocity. Higher values of radiation parameter, thermophoresis parameter, the microrotation increase near plane-surface and gradually diminishes far away from plane-surface. Profiles of temperature enhances with increasing the viscous dissipation parameter. Profiles of the concentration decreases by increasing the thermophoresis parameter and Schmidt number. Profiles of Skin friction and mass transfer rate decreases for magnetic field, thermal radiation and Schmidt number values.

Keywords: Thermophoresis MHD; Mass Transfer; Viscous Dissipation, Micropolar; Suction/injection; Heat Generation/Absorption.

1. Introduction

When pressure and temperature are held constant, non-Newtonian fluids have a nonlinear relationship between shear stress and deformation rate. Various industrial applications utilize such fluids, including thermal oil recovery, industrial pollution discharge, food processing, and polymer manufacturing, etc. Numerous applications of non-Newtonian boundary layers are found in industry, including fabrication, cooling of metallic plates, layering onto rigid substrates, and aerodynamic extrusion of plastic sheets. A wide range of factors have been considered in studies of such flows. Among the non-Newtonian fluids, micropolar fluids fall into this category. A micropolar fluid has a microstructure. Researchers have been interested in the study of micropolar fluids recently since Navier–Stokes calculations cannot accurately describe the features of fluids with suspended atoms. During the first century of the twentieth century, Eringen [1] presented a mathematical theory of liquid crystals, liquid crystals with ferro fluids and colloidal fluids based on the microfluid theory. Microrotation and local structures of fluid nanoparticles are being investigated by many researchers for their potential to demonstrate certain microeffects. Such fluids determined by spin inertia are capable of supporting the body and supporting stress moments. Among the microfluids, the micropolar fluid possesses microrotational effects and microrotational inertia. Because of its tiny structure, the micropolar is a foundation of the chemical Navier–Stokes model. Industrial processes rely heavily on micropolar fluids for a variety of purposes. A thermo-micropolar fluid theory was introduced by Eringen [2]. In the later studies of these fluids over a semi-infinite plate of

high temperature, many researchers focused on the following attributes. A homogeneous suspension of microparticles confirms the significant micropolar properties. Using occurrence variable heat source/sink, Kumar et al. [3] explored simultaneous solutions for micropolar fluid flow through a convective surface. According to Anantha et al. [4], a modified heat flux model provides an insight into ferroelectric fluid dissipation past slendering stretching surfaces. Chiu and Chou [5] examined the role of two-dimensional free convective micropolar fluid via vertical permeable surface. Through the use of suction and blowing, Hassanien and Gorla [6] have accomplished micropolar liquid heat transfer past a non-isothermal stretched sheet. Gorla [7] has investigated mixed convective micropolar liquid past a horizontal plate. More than that, several researchers in [8–15] have studied the unique qualities of micropolar fluid boundary layer flow across an infinite plate in presence of several parameters.

Several metallurgical and chemical engineering procedures have direct bearing on heat transport situation over a stretched sheet. Because of its practical significance, several researchers have investigated the flow across a stretchable surface at various stretchable velocities. The accuracy of the findings of a thermal management study may be severely impacted by the widespread underestimation and frequent disregard of radiation as a heat transfer method. One of the three ways in which energy may be transferred between objects of temperatures is by thermal radiation. The emission of electromagnetic waves from a substance is a defining feature of thermal radiation. In certain cases, the potential impact of radiation is high enough to warrant special consideration. When the surface temperature of an item or piece of technology is very high, it radiates a great deal of heat into the surrounding space. The scientific community has long recognized that in many industrial applications, the stretching is not strictly linear. Many studies have examined nonlinear stretching sheets for various fluid flows. Many technological processes rely on heat transmission, which is impacted by thermal radiation. This includes satellites, gas turbines, and numerous propulsion engines for airplanes, and spacecraft. Hossain and Alim [16] reported, free convective and heat radiation interacting along a vertical thin cylinder, utilizing Rosseland diffusion estimation. Natural convective incompressible liquid via an isothermal horizontal plate has been presented, by finite difference approach, as done by [17]. Abdel-naby et al. [18] proposed MHD radiative transient flow implication via a vertical plane assuming temperature gradient along its surface. Hossain [19] studied free magneto convective flow with varying wall temperature, taking into account the impact of Joule heating. Finite difference methods were used by Mamun et al. [20] to examine the impact of heat production on convective flow along vertical flat plane. Effects of dissipative ohmic heating on MHD flow down an inclined plane with a changing exterior temperature were analyzed by Palani and Kim [21] using Crank-Nicolson technique. According to the literature, MHD convective flow of micropolar fluid does not include thermophoresis. Rashed et al. [22] contributed mass transmission of a micropolar liquid across isothermal vertically planed, absorbed in a fervently and solutely stratified media. Eid et al. [23] reported a mathematical analyzation in heat transfer micropolar fluid flow over a permeable inclined surface, considering Dufour and magnetic effects. According to Rafique et al. [24], numerical solutions were obtained for micropolar nanofluid flow over inclined surfaces using the Keller box method.

Temperature-sensitive molecules moving in a liquid cause thermal gradients and the elements flow backwards according to the thermal gradients. This is thermophoresis. Natural convection relies heavily on thermophoresis forces due to lower liquid velocities. A loaded liquid element also boosts thermophoresis velocity permanently in the direction of a decreasing thermal gradient. It is common for fluids to play an important role in the development of industrial and engineering processes, including crystal growing and glass blowing, polymer extrusions, and metallurgical processes, among others. Temperature-dependent particle transfer from a hot surface to a cool surface occurs during the extrusion process, as well as the heated liquid stretching into a cooling system. Small particles, such as dust, exert force parallel to temperature gradients, called thermophoretic force, which causes these particles to move. Goren [25] explored thermophoresis in the context of thermodynamics. Determining the rate of deposit and demonstrating that significant variations in surface deposition can be produced by increasing temperature differentials were demonstrated by him. There is a strong correlation between radioactive thermophoretic deposition particles and nuclear reactor accidents. It was found that particle free layers are observed around hot surfaces as a result of thermophoresis, since particles are transferred towards cold surfaces via thermophoresis, while particles residing on a hot surface are also not transferred, according to Goldsmith and May [26]. By combining thermophoretic movement with thermal radiation, Abbas et al. [27] have studied two-dimensional free-forced convection flow of optically dense non-Newtonian gray fluid. An analysis of the flow of MHD hydrothermal hydroslides along a permeable flat surface with variable heat source/sink and thermal conductivity was carried out by Das et al. [28]. Moreover, Swain et al. [29] demonstrate how chemical reactions are impacted by constant internal heat sources and heat sinks. Over a permeable horizontal surface, variable thermophoretic forces, viscous heat dissipation, and dependent thermal conductivity were examined [30-37]. Impacts of the work carried out and contributed to in [38-42].

By witness of review of literature such analysis is not performed for micropolar fluid with thermophoretic effect. The advancement of energy is one of the most important topics in our century due to its industrial and technological applications. This analysis presents a numerical analysis of the flow of electrically conducted micropolar fluid over a vertical stretching surface as a function of thermal conductivity. Heat source and thermal radiation implications are considered. In response to the literature review, our study examines the impact of thermophoretic force on two-dimensional MHD micropolar fluid flow. The goal of the article is to examine the interplay between thermophoresis and heat generation/absorption in the steady magnetohydrodynamic convective micropolar fluid past an inclined radiative isothermal surface. Finally, graphs of micropolar fluid velocity, micropolar angular momentum, micropolar temperature, micropolar concentration, skin friction, Nusselt and Sherwood number sketches are plotted and tabularized for all their aspects are deliberated. Section 2 shows the mathematical formulation of the proposed model. The procedure for generating entropy is presented in Section 3. The proposed model is numerically solved in Section 4. A physical discussion of the results of the present analysis can be found in Section 5 of this report. In Section 6, we present the final results of our analysis.

2. Mathematical Formulation

An incompressible flow in a micropolar fluid, with thermophoresis particle deposition on a vertical stretching surface, as a steady convective MHD free flow This is achieved by assuming a very small magnetic Reynolds number and neglecting the transverse magnetic field B_0 along the y-axis. Hall and ion slip effects may also be ignored due to the weak magnetic field applied. Surfaces that stretch have linear velocity U_0. The sheet is stretched proportionally to the distance from the origin by applying two equal and opposite forces along the x-axis, $x = 0$ (see Fig. 1). Compared to Fourier's and Fick's laws, the Soret and Dufour effects are not taken into account because they are of a smaller magnitude. As for the usual boundary approximations, these are the governing equations: (see Mondal [46]):

(i) Continuity:

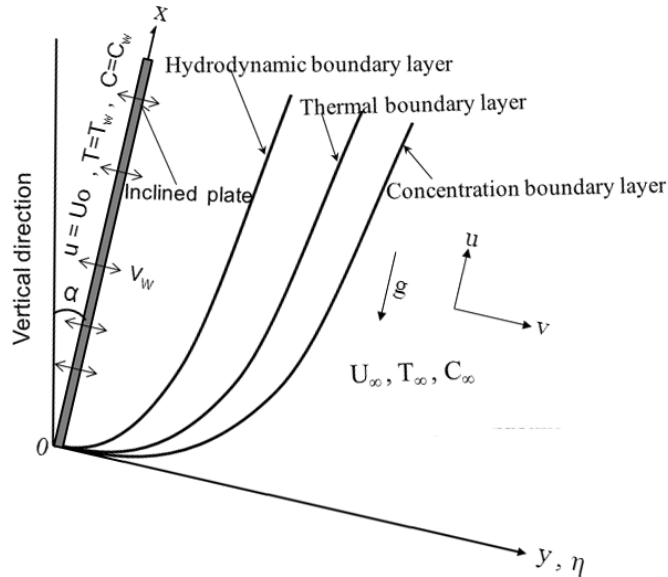$$\frac{\partial u}{\partial x} + \frac{\partial u}{\partial y} = 0, \qquad (1)$$

Fig. 1. Physio-coordinate diagram for the physical model.

(ii) Momentum:

$$u\frac{\partial u}{\partial x} + v\frac{\partial u}{\partial y} = \nu\frac{\partial^2 u}{\partial y^2} + g\beta_T\left(T - T_\infty\right)\cos\alpha + g\beta_C\left(C - C_\infty\right)\cos\alpha + K_1\frac{\partial N}{\partial y} - \frac{\sigma B_0^2}{\rho}u,$$

(2)

(iii) Angular momentum:

$$G_1\frac{\partial^2 N}{\partial y^2} - 2N - \frac{\partial u}{\partial y} = 0,$$

(3)

(vi) Energy:

$$u\frac{\partial T}{\partial x} + v\frac{\partial T}{\partial y} = \frac{k}{\rho c_p}\frac{\partial^2 T}{\partial y^2} - \frac{1}{\rho c_p}\frac{\partial q_r}{\partial y} + \frac{\nu}{c_p}\left(\frac{\partial u}{\partial y}\right)^2 + \frac{Q_0}{\rho c_p}(T - T_\infty),$$

(4)

(v) Concentration:

$$u\frac{\partial C}{\partial x} + v\frac{\partial C}{\partial y} = D\frac{\partial^2 C}{\partial y^2} - \frac{\partial}{\partial y}(V_T C)$$

(5)

These are the model's boundary conditions:

$$u = U_0,\ v = \pm v_w(x),\ C = C_w, N = -\frac{1}{2}\frac{\partial u}{\partial y},\ T = T_w,\ \text{at } y = 0$$

$$u \to U_\infty,\ C \to C_\infty, N \to 0,\ T \to T_\infty,\ \text{as } y \to \infty$$

(6)

The heat flux radiation q_r (Brewster [47]) is specified by:

$$q_r = -\frac{4\sigma_*}{3k_*}\frac{\partial T^4}{\partial Y}$$

(7)

where

$$T^4 \cong 4T_\infty^3 T - 3T_\infty^4$$

(8)

By using (7) and (8), Eq. (4) gives:

$$u\frac{\partial T}{\partial x} + v\frac{\partial T}{\partial y} = \frac{k_e}{\rho c_p}\frac{\partial^2 T}{\partial y^2} - \frac{16\sigma T_\infty^3}{3\rho c_p k_1}\frac{\partial^2 T}{\partial y^2} + \frac{\nu}{c_p}\left(\frac{\partial u}{\partial y}\right)^2 + \frac{Q_0}{\rho c_p}(T - T_\infty)$$

(9)

Temperature-dependent thermophoretic velocity is expressed as follows (Goren [25]):

$$V_T = -kv\frac{\nabla T}{T_{ref}} = \frac{-kv}{T_{ref}}\frac{\partial T}{\partial y}$$

(10)

where $k \in [0.2\text{-}1.2]$ (Batchelor and Shen [37]) and is explained by (Talbot et al. [38]):

$$k = \frac{2Cs\left(\lambda_g / \lambda_p + C_t K_n\right)\left[1 + K_n\left(C_1 + C_2 e^{-C_3 / K_n}\right)\right]}{\left(1 + 3C_m K_n\right)\left(1 + 2\lambda_g / \lambda_p + 2C_t K_n\right)} \tag{11}$$

A thermophoretic parameter τ is defined as (Mills et. al [39]):

$$\tau = \frac{-k\left(T_w - T_\infty\right)}{T_r} \tag{12}$$

Equation (1) is gratified by a stream function ψ as:

$$u = \frac{\partial \psi}{\partial y}, \quad v = -\frac{\partial \psi}{\partial x}.$$

A dimensionless variable is defined as follows (El-Arabawy [15]):

$$\eta = \left(\frac{U_0}{2\nu x}\right)^{1/2} y, \ \psi = \left(2\nu U_0 x\right)^{1/2} f(\eta), \ \theta(\eta) = \frac{T - T_\infty}{T_w - T_\infty}, \ \phi(\eta) = \frac{C - C_\infty}{C_w - C_\infty},$$
$$u = U_0 f'(\eta), v = -\sqrt{\frac{2\nu U_0}{x}}\left[f(\eta) - \eta f'(\eta)\right], N = \left(\frac{U_0}{2\nu x}\right)^{1/2} U_0 g(n) \tag{13}$$

Taking note of Eq. (13), corresponding modified governing Eqs. (2), (3), (5) and (9) conceivably expressed as:

$$f''' + ff'' - Mf' + Gr\theta\cos\alpha + Gc\phi\cos\alpha + Kg' = 0 \tag{14}$$

$$Gg'' - 2(2g + f'') = 0 \tag{15}$$

$$(3R + 4)\theta'' + 3R\Pr Ec(f'')^2 + 3RQ\theta + 3R\Pr f\theta' = 0 \tag{16}$$

$$\phi'' + Sc(f - \tau\theta')\phi' - Sc\tau\theta''\phi = 0 \tag{17}$$

where

$$M = \left(\frac{\sigma U_\infty}{\rho}\right)^{1/2} B_0, \quad G = \frac{G_1 U_0}{2\nu x}, \quad Gr = \frac{g\beta_T\left(T_w - T_\infty\right)2x}{U_0^2}, \quad Gc = \frac{g\beta_c\left(C_w - C_\infty\right)2x}{U_0^2},$$
$$K = \frac{K_1}{\nu}, \quad \Pr = \frac{\nu}{K}, \quad R = \frac{kk_e}{4\sigma_s T_\infty^3}, \quad Ec = \frac{U_0^2}{c_p\left(T_w - T_\infty\right)}, \quad Q = \frac{Q_0}{\rho c_p}, \quad Sc = \frac{\nu}{D}, \quad \tau = -\frac{k\left(T_w - T_\infty\right)}{T_r}.$$

Boundary conditions (6) after transformation are:

$$f(0) = f_w, \ \phi(0) = 1, f'(0) = 1, \ \theta(0) = 1, g(0) = -\frac{1}{2}f''(0)$$
$$f(\infty) = 0, \ \phi(\infty) = 0, g(\infty) = 0, \ \theta(\infty) = 0 \tag{18}$$

The skin friction C_f, the couple stress C_m, heat and mass transfers ($q_w(x)$, Sh_x) from the wall-surface assumed by:

$$C_f \operatorname{Re}_x^{-1/2} = \frac{\tau_w}{(1/2)\rho U_0^2} = 2f''(0), \ \tau_w = \mu\left(\frac{du}{dy}\right)_{y=0} \tag{19}$$

$$Nu_x \operatorname{Re}_x^{-1/2}\left(\frac{3R}{3R + 4}\right) = \frac{q_w(x)}{\lambda\left(T_w - T_\infty\right)} = -\frac{1}{2}\theta'(0); q_w(x) = -\lambda\left(\frac{\partial T}{\partial y}\right)_{y=0} - \frac{4\sigma}{3k_1}\left(\frac{\partial T^4}{\partial y}\right)_{y=0} \tag{20}$$

$$Sh_x \operatorname{Re}_x^{-1/2} = -\frac{J_s}{U_0 C_\infty}; J_s = -D\left(\frac{\partial C}{\partial y}\right)_{y=0} = \phi'(0) \tag{21}$$

where $\operatorname{Re}_x = U_0 x/\nu$ is the local Reynolds number.

3. Investigation of Entropy Generation

In the modern era, researchers and engineers are increasingly focused on developing techniques to minimize energy waste [43-45]. Entropy, a novel concept, offers potential to control this wastage and improve system performance. This research explores how fluid friction, mass transfer, and heat transfer contribute to entropy generation, ultimately presenting A measure of the rate at which micropolar fluids generate volumetric entropy:

$$E_{gen} = E_a + E_b + E_c$$

where

$$E_a = \frac{k_e}{T_\infty^2}\left(1 - \frac{16\sigma^* T_\infty^3}{3k^* k}\right), E_b = -\left(2N + \frac{\partial u}{\partial y}\right), E_c = \frac{\mu}{T_\infty}\left(\frac{\partial u}{\partial y}\right)^2$$

The rate at which dimensionless entropy is generated is defined as follows:

$$E_s = \frac{k_e\left(T - T_\infty\right)^2}{T_\infty^2}$$

Equation (13) can be represented in the dimensionless form as by entropy generation characteristics rate (E_1):

$$E_G = \frac{E_{gen}}{E_s} = \mathrm{Re}_x\left(3R + 4\right)\theta^2 + \frac{2Br\,\mathrm{Re}_x}{\delta}\left(g^2 + gf\right) + \frac{Br\,\mathrm{Re}_x}{\delta}Ecf'^2$$

and

$$E_1 = \mathrm{Re}_x\left(3R + 4\right)\theta'^2$$

Bejan number (Be) is the ratio between entropy generated by heat transfer (E_1) and total entropy generation (E_G), i.e.:

$$Be = \frac{E_1}{E_G}$$

Linear thermal radiation parameters are defined as dimensionless parameters in the above equation:

$$R = \frac{kk_e}{4\sigma_s T_\infty^3},$$

Reynold number $\mathrm{Re}_x = U_0 x / \nu$, Brinkman number $Br = \mathrm{Pr} \times Ec$, and temperature difference parameter $\delta = \dfrac{T_w - T_\infty}{T_\infty}$.

4. Method of Solution

Runge-Kutta iterations of the 4th order combined with the shooting strategy are accustomed solve the system of ordinary differential equations (14) through (17), which are constrained by the boundary conditions (18). For all scenarios, we found that a step size of $\Delta \eta = 0.01$ was sufficient as a criteria convergence 10^{-6}. The findings for the flow field and other physical parameters are reached, and the outcomes are graphically illustrated in Figs. 2 to 11. The flow chart of the process is shown below:

```
                    ┌──────────────────────────────┐
                    │ Boundary Value Problem (BVP)  │
                    └──────────────────────────────┘
                                  │
                    ┌──────────────────────────────┐
                    │  Initial Value Problem (IVP)  │
                    └──────────────────────────────┘
                                  │
                    ┌──────────────────────────────┐
                    │     Choose the missing        │
                    │     initial conditions        │
                    └──────────────────────────────┘
                                  │
     ┌──────────────────────┐    ┌──────────────────────────┐
     │ Solve IVP by 4th order│◄──│ Initial guesses are      │
     │ Runge-Kutta method    │   │ modified by Newton' method│
     └──────────────────────┘    └──────────────────────────┘
                  │                            ▲
┌────────────────────┐ ┌──────────────┐ ┌───────────────────────┐
│ If boundary        │◄│ Calculate    │►│ If boundary residuals │
│ residuals are less │ │ boundary     │ │ are greater than      │
│ than tolerance     │ │ residuals    │ │ tolerance             │
└────────────────────┘ └──────────────┘ └───────────────────────┘
         │
   ┌──────────────┐
   │ Final        │
   │ solutions    │
   └──────────────┘
```
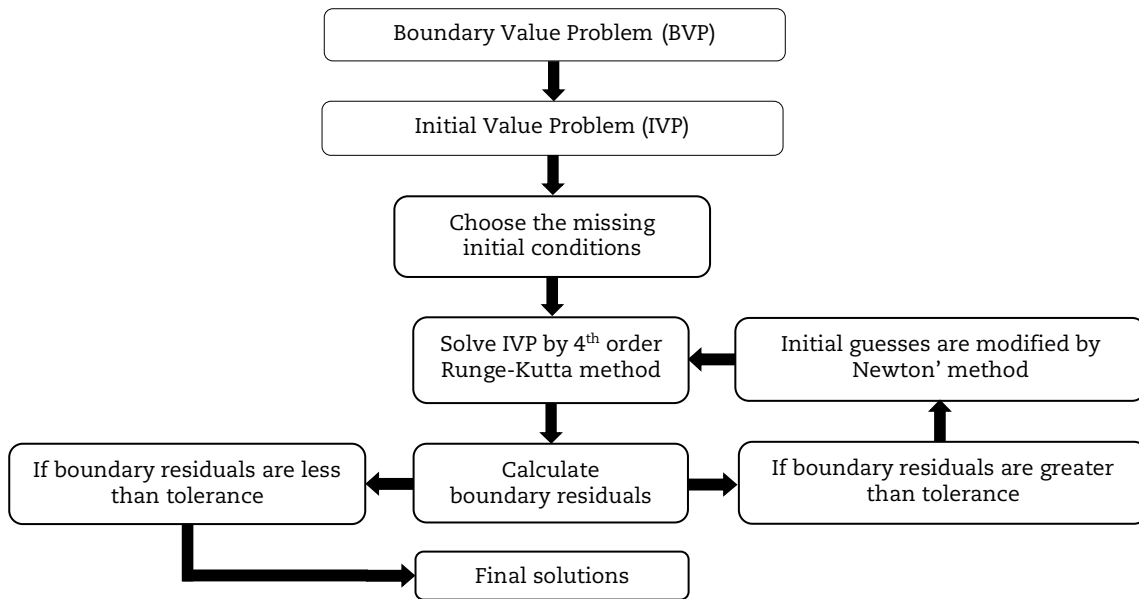
The R-K technique, along with the shooting process, approach is made up of a number of different processes that is carried out repeatedly in order to derive the solutions. In order to get a set of first order derivatives, the boundary conditions and the governed equations are combined together:

$$[f, f', f'', g, g', \theta, \theta', \phi, \phi'] = [f_1, f_2, f_3, f_4, f_5, f_6, f_7, f_8, f_9]$$

The boundary conditions are:

$$f_1 = f_w, f_2 = 1, f_4 = -\frac{1}{2}f_3, f_6 = 1, f_8 = 1 \quad \text{at} \quad \eta = 0 \tag{22}$$

$$f_1 = f_4 = f_6 = f_8 = 1 \quad \text{at} \quad \eta = \infty \tag{23}$$

$$\left.\begin{array}{l} f_3' = Mf_2 - f_1 f_3 - Gr f_6 \cos\alpha - Gc f_8 \cos\alpha - K f_5 \\ f_5' = \dfrac{2[2f_4 + f_3]}{G} \\ f_7' = -[3R\Pr f_1 f_7 + 3R\Pr Ec] \\ f_9' = Sc\tau f_7 f_8 - Sc f_9 [f_1 - \tau f_7] \end{array}\right\} \tag{24}$$

Mathematica is strong mathematical computing and visualization program. Its benefits include:

- Mathematica can do algebraic manipulations, calculus, statistics, and numerical analysis.
- Data analysis, visualization, and programming is possible.
- The Mathematica interface is simple to use and lets users enter and alter mathematical equations using normal language.
- Mathematica's tutorials, examples, and help files make it simple to learn and use.
- Mathematica's extensive user base makes online assistance easy.

5. Results and Discussion

Equations (14) to (17) form a third- and second-order extremely non-linear linked boundary value problem. The Runge-Kutta algorithm for 4th order integration has been employed with the shooting iteration method. With the exception of the distinct characteristics shown in Figs. 2–11 and Tables 1 and 2, all of these values remain constant during, the duration of the research. Very recent works [52-56] explored more applications related to the present analysis.
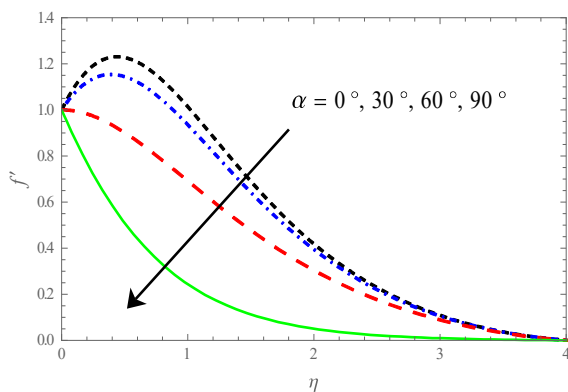
Fig. 2(a). Plots for velocity $f'(\eta)$ on α.
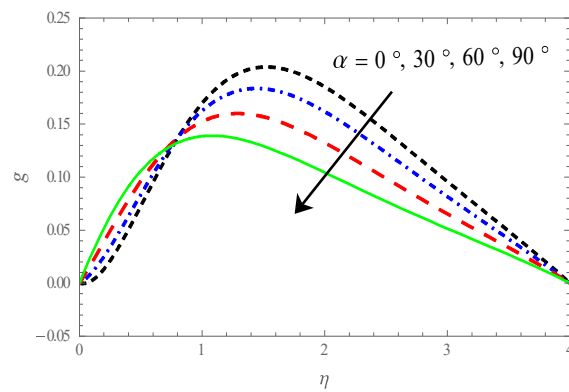
Fig. 2(b). Plots for microrotation g(η) on α.
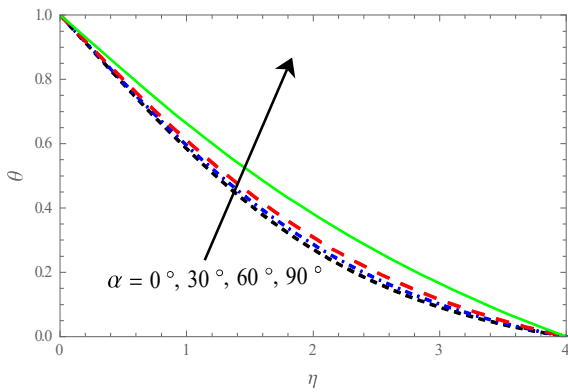
Fig. 2(c). Plots for temperature $\theta(\eta)$ on α.
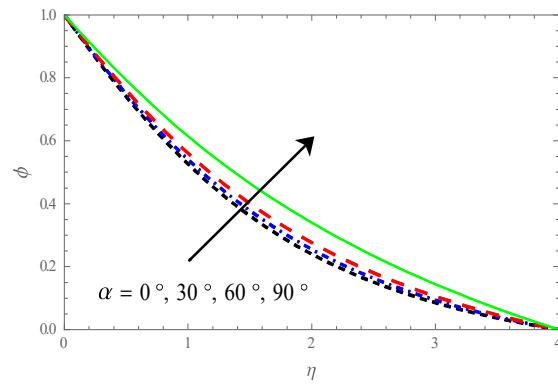
Fig. 2(d). Plots for concentration $\phi(\eta)$ on α.
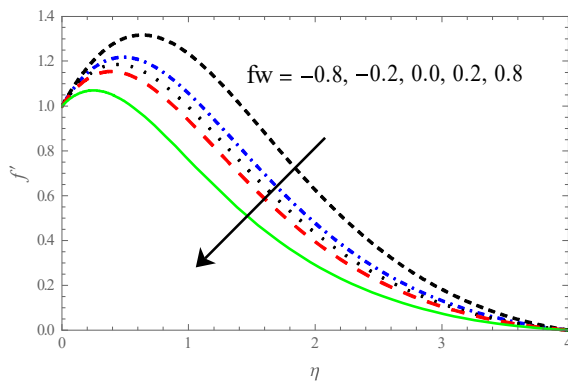
Fig. 3(a). Plots for velocity on fw.
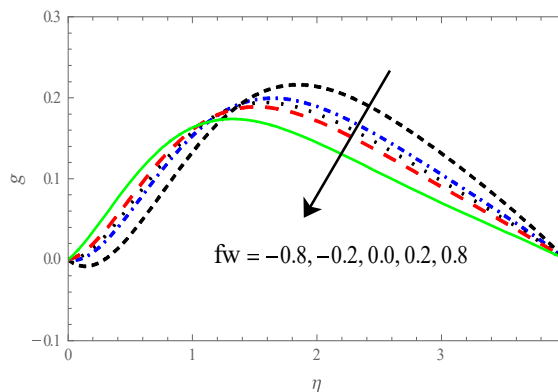
Fig. 3(b). Plots for microrotation g(η) on fw.
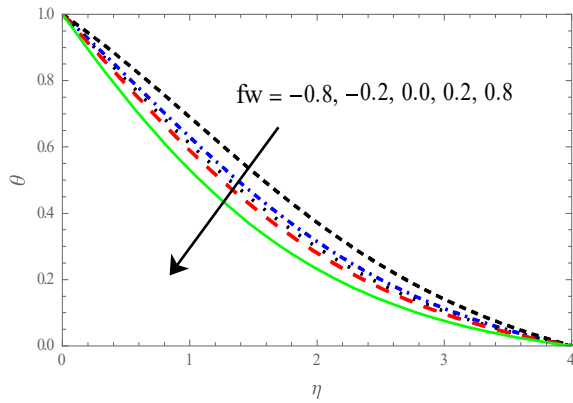
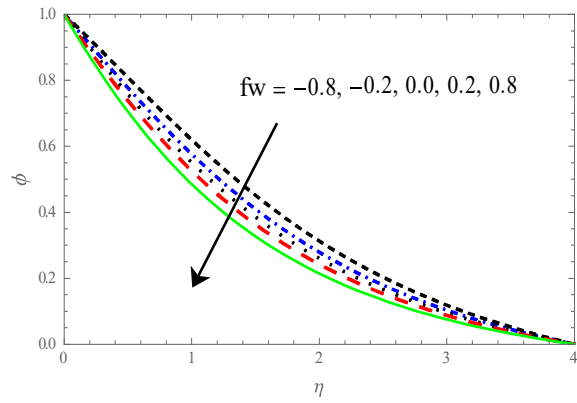**Fig. 3(c).** Plots for temperature $\theta(\eta)$ on fw.

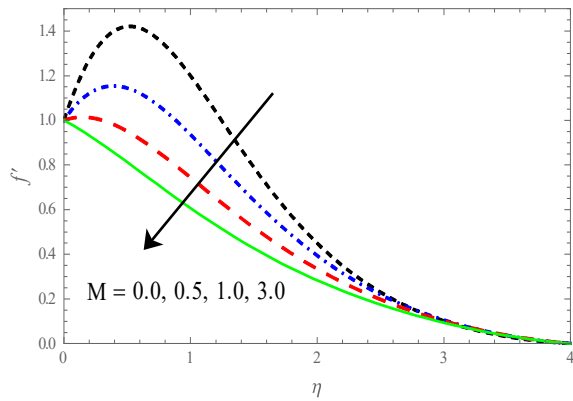**Fig. 3(d).** Plots for concentration $\phi(\eta)$ on fw.

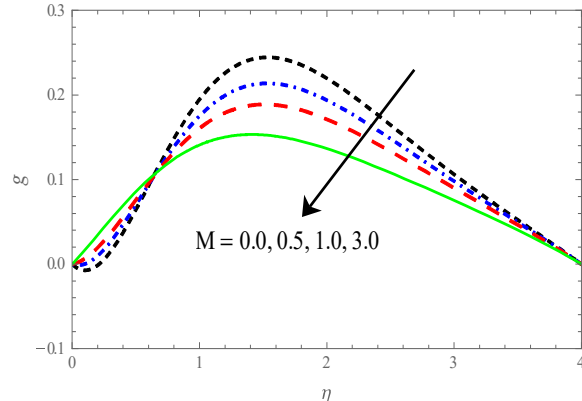**Fig. 4(a).** Plots for velocity on M.

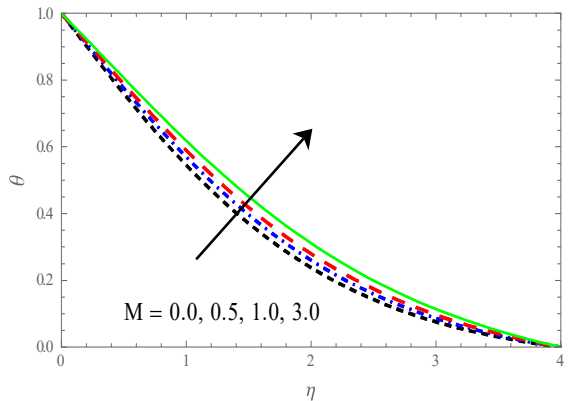**Fig. 4(b).** Plots for microrotation $g(\eta)$ on M.

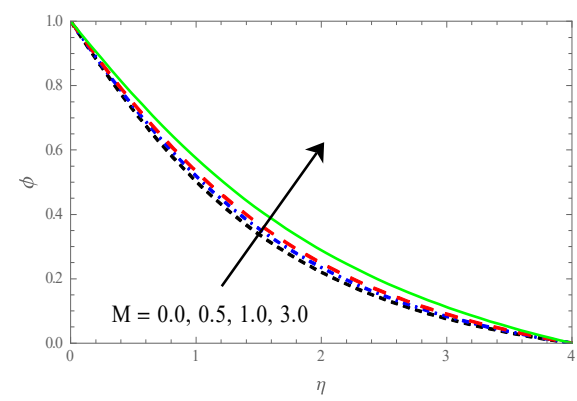**Fig. 4(c).** Plots for temperature $\theta(\eta)$ on M.

Fig. 4(d). Plots for concentration $\phi(\eta)$ on M.

Figures 2(a) to 2(d) illustrate $f'(\eta)$, $g(\eta)$, $\theta(\eta)$ and $\phi(\eta)$ distributions depending on the degree of inclination. Figure 2(a) performances as inclination angle raises, the velocity profiles get flatter. Figure 2(b) shows that as the angle of inclination rises, the microrotation is greatest nearer the wall and diminishes farther away. It can be shown in Figs. 2(c) and 2(d) that when the angle of tilt rises, both temperature and concentration distributions raise.

Varied suction parameter values, result in varied $f'(\eta)$, $g(\eta)$, $\theta(\eta)$ and $\phi(\eta)$ distributions, as exhibits in Figs. 3(a) to 3(d). Increasing fw, considers in Fig. 3(a), causes a drop in $f'(\eta)$ distributions. As fw is raised, the microrotation is shown to grow close to the porous plate and subsequently to decrease at farther distances. Figures 3(c) and 3(d) exhibits the fw is heightened, the temperature and concentration are both lowered. As a physical measure, increase fw indicates fw < 0, the mass transfer at the sheet due to suction. For larger values of S, the fluid is moving at a higher velocity at $\eta = 0$. In convergence with the boundary condition at $\eta = 4$, which the fluid velocity converges $\eta \to \infty$.

Figures 4(a), 4(b), and 4(c) exhibit the changes in velocity, microrotation, and temperature as a function of M. Figure 4(a) displays unmistakably that as M intensifications, velocity profiles decrease. Figure 3(b) confirmations, as the magnetic parameter rises, the microrotation is greatest nearer the wall and diminishes farther away. Figures 4(c) and 4(d) show that when the magnetic parameter is amplified, $\theta(\eta)$ and $\phi(\eta)$ both rise. Physically, the fluid, when Lorentz forces are present and M is rising, has less velocity. Increasing magnetic values corresponds to a smaller velocity and hence, a thinner boundary layer hydrodynamically. Meanwhile, microrotation profiles show the opposite with rising M values. Additionally, the magnetic field exerts a greater impact on translational velocity than micro rotational velocity.
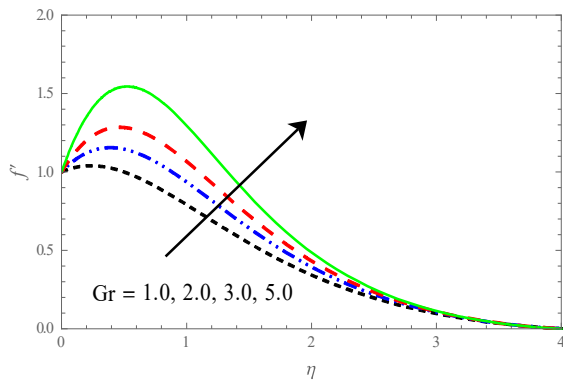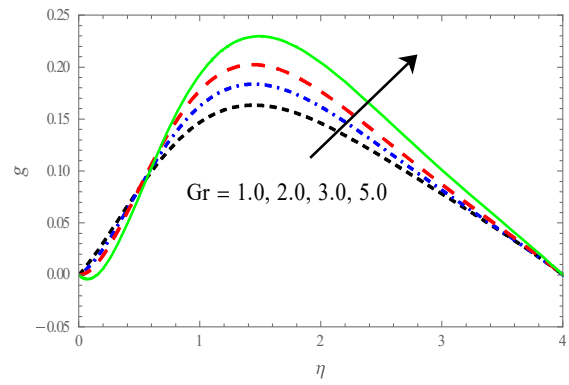
Fig. 5(a). Plots for velocity $f'(\eta)$ on Gr.

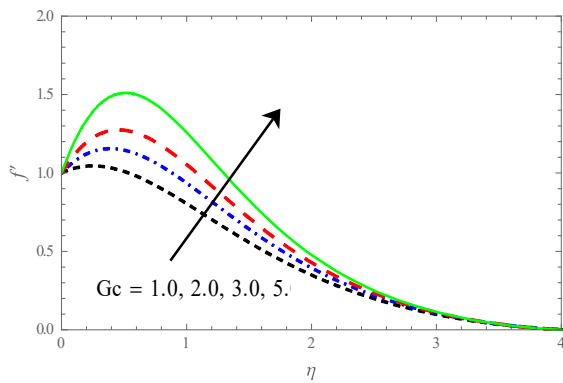**Fig. 5(b).** Plots for microrotation g(η) on Gr.

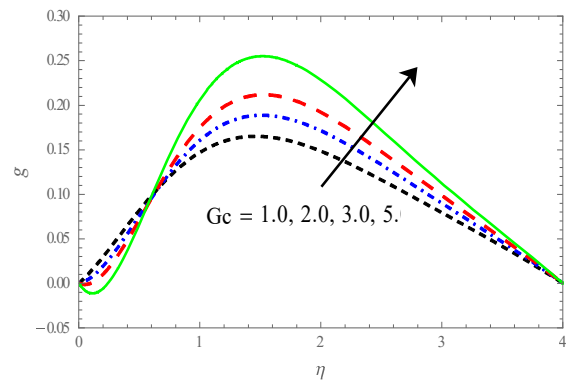**Fig. 6(a).** Plots for velocity $f'(\eta)$ on Gc.

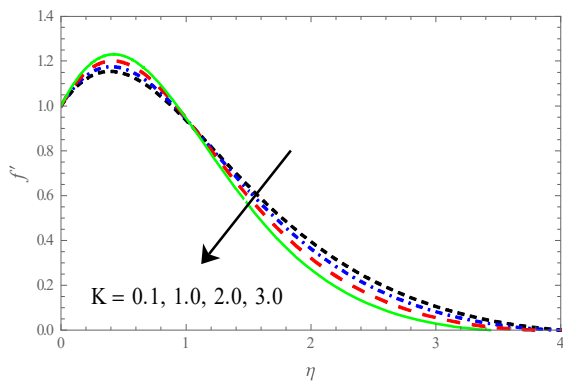**Fig. 6(b).** Plots for microrotation g(η) on Gc.
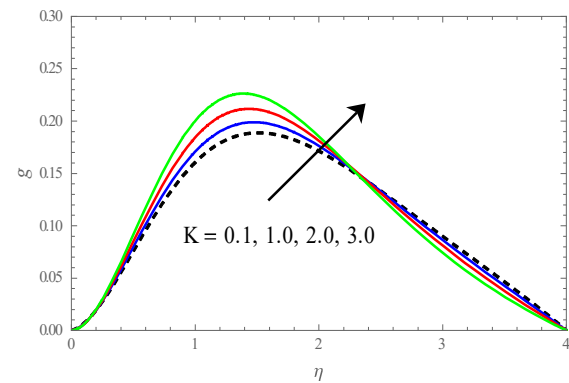
Fig. 7(a). Plots for velocity $f'(\eta)$ on K.
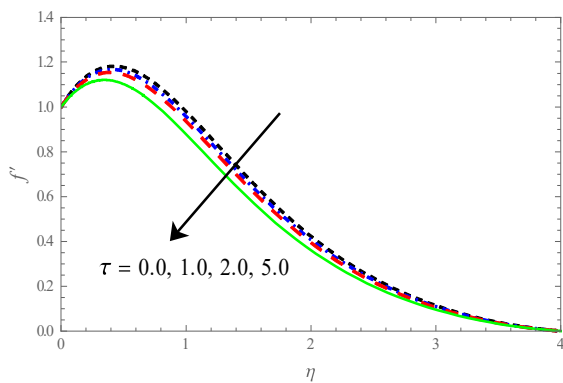
Fig. 7(b). Plots for microrotation g(η) on K.
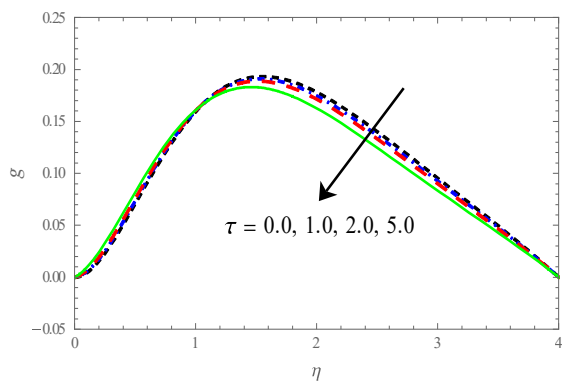
Fig. 8(a). Plots for velocity $f'(\eta)$ on τ.

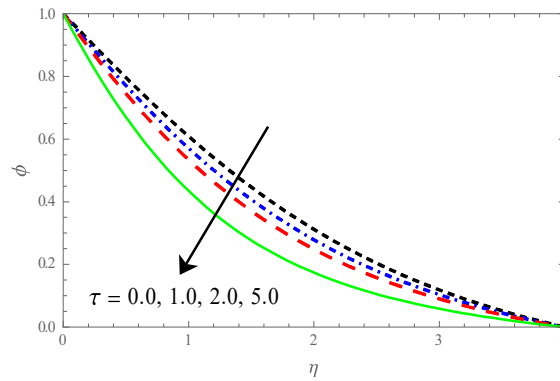**Fig. 8(b).** Plots for microrotation g(η) on τ.

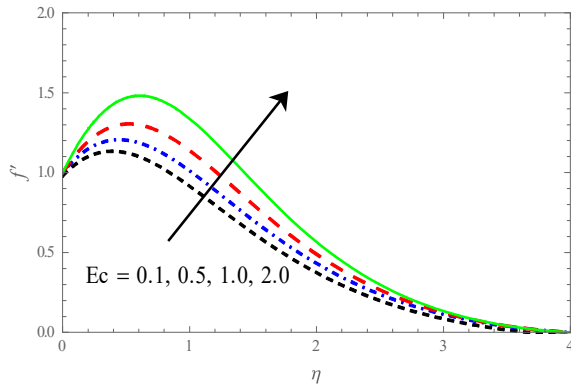**Fig. 8(c).** Plots for concentration $\phi(\eta)$ on τ.

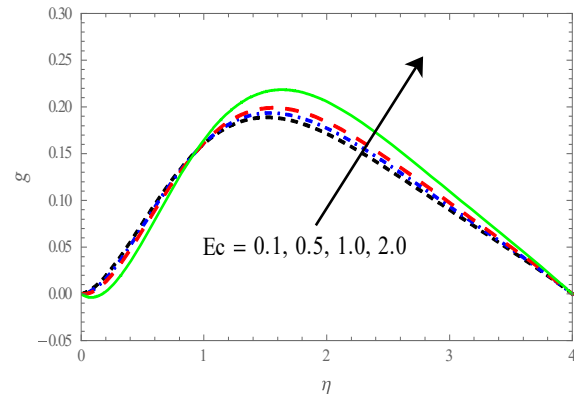**Fig. 9(a).** Plots for velocity $f'(\eta)$ on Ec.

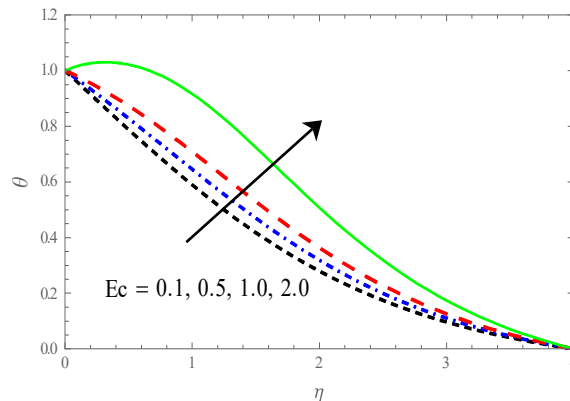**Fig. 9(b).** Plots for microrotation g(η) on Ec.

Fig. 9(c). Plots for temperature $\theta(\eta)$ on Ec.

Figures 5 and 6 demonstrate the velocity and microrotation distributions for various values of 'Gr' and 'Gc'. Increasing Gr or Gc is found to enhance velocity values, while decreasing microrotation close to the porous plate and increasing it farther away from the permeable plate is seen. It refers to the ratio between the buoyancy force of fluid density variation (induced by temperature differences) and the restraining force of fluid viscosity.

Figures 7(a)-(b) show an influence of varying the coupling constant on velocity and microrotation curves. Increasing the coupling constant is shown to result in a rise in velocity (Fig. 7(a)) and the result, the boundary layer thickness enhances. Physically, A high K value corresponds to a lower viscosity and a weaker rotation of the particles. Variations of the fluid's maximum velocity at $\eta = 0$, are associated with distinct K values. As $\eta \to \infty$, the fluid settles at the boundary as its velocity and microrotation converge. As K rises, the data reveal that microrotation progresses close to the porous plate and downgrades at farther distances.

Figures 8(a)-(c) displays τ variance on $f'(\eta)$, g(η) and $\phi(\eta)$ distributions. Raising the thermophoretic parameter results in higher velocity. Microrotation rises the nearer plate and decreases at further distances, perceived in Fig. 8(b). Figure 8(c) exemplifies, when τ is raised, so does the concentration profile. Temperature-dependent measurements of soot flow velocity in microgravity. Temperature gradients force small particles toward colder regions. A significant effect of thermophoretics on momentum and concentration boundary layers can be expected.

The distributions of $f'(\eta)$, g(η), $\theta(\eta)$ and $\phi(\eta)$ for Eckert number Ec, are plotted in Figs. 9(a)-(c). The velocity is shown to grow as the Eckert number Ec becomes larger. Figure 9(b) exhibits, when the Eckert number rises, microrotation increases close to the plate and decreases at farther distances. Eckert number rises, so does the temperature profile, seen in Fig. 9(c). The frictional heating of the particles leads to higher Ec values due to greater heat generation in the fluid. A higher temperature is also apparent.
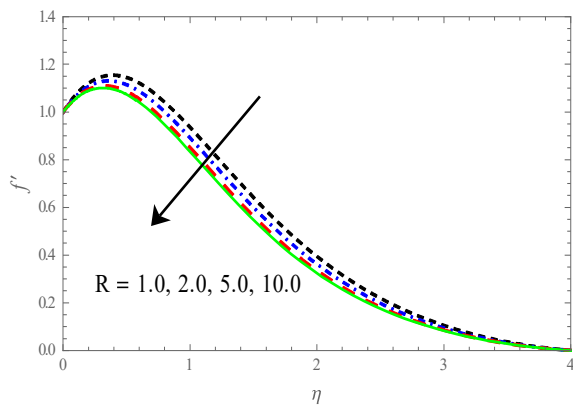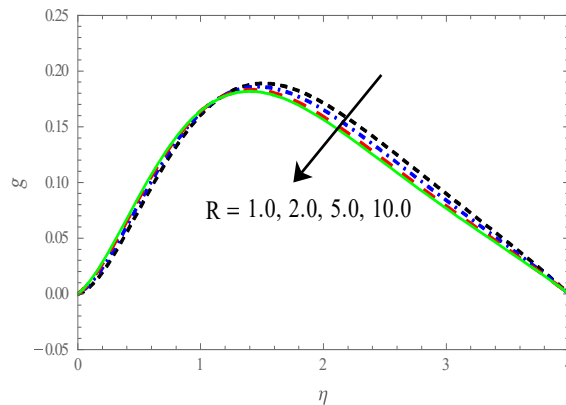
Fig. 10(a). Plots for velocity $f'(\eta)$ on R.

Fig. 10(b). Plots for microrotation g(η) on R.
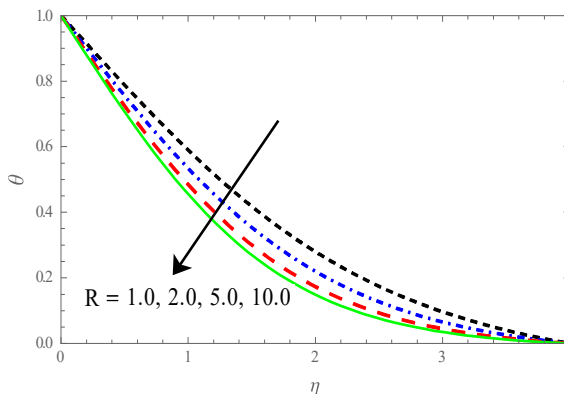
Fig. 10(c). Plots for temperature $\theta(\eta)$ on R.
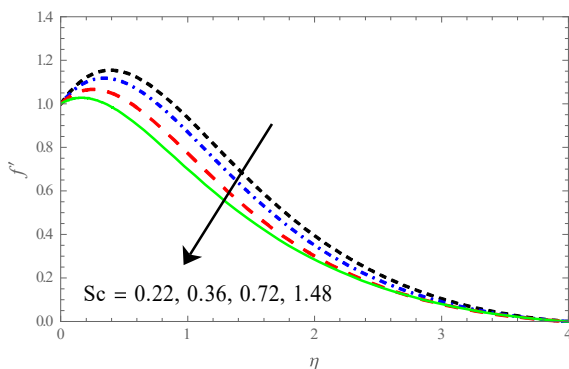
Fig. 11(a). Plots for velocity $f'(\eta)$ on Sc.
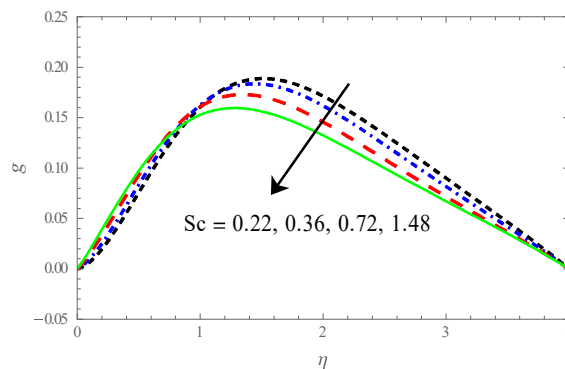
Fig. 11(b). Plots for microrotation g(η) on Sc.
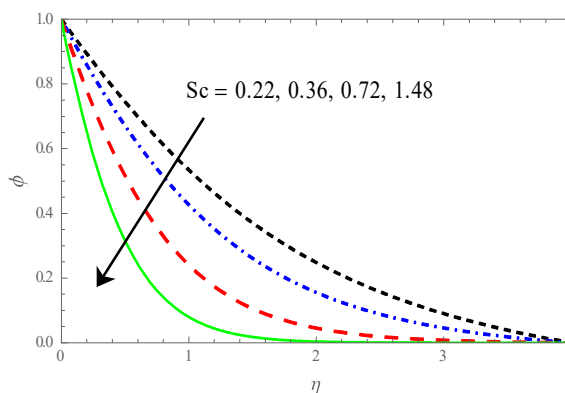
Fig. 11(c). Plots for concentration $\theta(\eta)$ on Sc.

Figure 10 displays velocity and microrotation patterns vs thermal radiation parameter R. Radiation parameter is heightens; a more even distribution of velocities is seen over the boundary layer. The findings also reveal that when R rises, microrotation on the isothermal plate improves close to the plate and decreases far away. when can be seen in Fig. 10(c), when R heightens; $\theta(\eta)$ profiles decay. It is expected to follow that an increase in R will result in a decline in the average Rosseland absorption coefficient and, therefore, a decline in temperature.

Table 1. Values of C_f, Nu_x and Sh_x for distinct parameters for α = 30°, G = 2.0, R = 1.0, Ec = 0.1, τ = 2.0, Sc = 0.22, Pr = 0.71.

Gr	Gc	M	K	C_f	Nu_x	Sh_x
2.0				1.147732	0.427590	0.555509
3.0				1.703161	0.423660	0.571029
5.0				2.751752	0.415802	0.592628
	2.0			1.147734	0.427590	0.555509
	3.0			1.167204	0.421598	0.569727
	5.0			2.677112	0.418125	0.589552
		1.5		1.565882	0.455373	0.579184
		1		1.147731	0.427590	0.555509
		3.0		1.128582	0.368161	0.502163
			0.1	1.147732	0.427590	0.555509
			1.0	1.223312	0.425791	0.555505
			2.0	1.315751	0.422981	0.555503

Table 2. Values of C_f, Nu_x and Sh_x for distinct parameters for α = 30°, G = 2.0, Gr = Gc = 2.0, K = 0.1, Pr = 0.71, and M = 1.

R	Ec	τ	Sc	C_f	Nu_x	Sh_x
1.0				1.147732	0.427590	0.555509
2.0				1.067781	0.498186	0.577004
5.0				1.029362	0.534942	0.588731
	0.1			1.147735	0.427590	0.555509
	0.3			1.235952	0.299285	0.509175
	0.5			1.338162	0.149012	0.455137
		1.0		1.189622	0.428641	0.489146
		2.0		1.147731	0.427590	0.555509
		3.0		1.107661	0.426549	0.624089
			0.22	1.147732	0.427590	0.555509
			0.3	1.021182	0.423624	0.747992
			0.48	1.015261	0.421152	0.868317

Table 3. Comparison of $-f''(0)$ and $g'(0)$ with Ref. [45] for M = 0, K = 0.2 and g = 2.0.

f_w	$-f''(0)$	$g'(0)$	$-f''(0)$	$g'(0)$
	Ref. [15]		Present study	
-0.7	0.278827	0.236917	0.278785	0.236785
-0.4	0.404227	0.286997	0.404357	0.286589
-0.2	0.504059	0.321165	0.504098	0.321568
0.0	0.616542	0.355330	0.616428	0.355457
0.2	0.741521	0.389278	0.741236	0.389147
0.4	0.877517	0.422223	0.877263	0.4222123
0.7	1.099430	0.468923	1.098712	0.468758

Table 4. Comparison of $-\theta'(0)$ with Ref. [15] for Ec = 0.02, f_w = 0, M = 0, R = ∞, K = 0.2, g = 2.0, Q = 0.0 and ϕ = 0.

Pr	$-\theta'(0)$ (Ref. [15])	$-\theta'(0)$ (Present study)
0.733	0.501327	0.501299
7.0	1.931150	1.931023
10	2.337000	2.336988
20	3.360750	3.360692
50	5.380040	5.380002

Figure 11 displays the velocity and microrotation curves as a function of Schmidt number Sc. When Sc is raised, the boundary layer's translational velocity rises. As Sc rises, it also seems that microrotation increases close to the plate but decreases at farther distances. Physically, Temperature layer and mass transfer boundary layer are related by Schmidt number.

The C_f, Nu_x and Stanton number are presented in Tables 1 and 2 for distinct values. Table 1 presents C_f, Nu_x values rises with increasing of the 'Gr' and 'Gc' and coupling constant, while they diminish with growing 'M' parameter. The Nusselt number decreases as increase thermal Grashof number and solutal Grashof number and coupling constant, is noted. In addition, from Table 2, increase the values of R, Ec, τ and Sc decrease the values of C_f and Stanton number, while upsurge in Nusselt number by growing in Eckert number values, thermophoretic parameter and Schmidt number is noted.

Previous numerical findings reported by El-Arabawy [15] were utilised to validate the aforementioned numerical technique. Tables 3 and 4 exhibit side-by-side comparisons of wall velocity, microrotation, and temperature slope. When compared, the findings show a great deal of uniformity.

6. Concluding Remarks

The mixture of convection and mass transfer in micropolar fluids across a permeable inclined isothermal surface owing to the effects of thermophoresis were reported. Partial differential equations generated by similarity transformations were converted into ordinary differential equations through similarity transformations. Skin friction, heat and mass transfer, near inclined isothermal plate, and the overall flow characteristics were determined by numerically solving the governing equations

using the R-K 4ᵗʰ order approach. Main conclusions from the current research are:

- The resultant velocity declines by any increase in parameters α, fw, M, K, τ, R and Sc.
- Velocity component and its boundary layer thickness raise with increasing values of Gr, Gc and Ec.
- For micro-rotation, higher values of α, fw, M K, R, τ, Ec and Sc, increases near the wall-surface and gradually diminishes far away from the wall-surface.
- The microrotation distributions improves with higher values of Gr, Gc and Ec.
- Profiles of Temperature heightens with a rise in angle of inclination α, magnetic parameter M and Eckert number Ec and leads to improves thermal boundary layer whereas reduces with increasing in radiation parameter R and leads to thickens the thermal layer.
- Mass transfer function heightens with rise in angle of inclination α and magnetic parameter M whereas decreases with increasing in thermophoresis parameter τ and Schmidt number Sc.
- Profiles of Skin friction coefficient and rate of mass transfer increments with intensification in Gr, Gc, K and Ec owing to rise but decreases for the values of M, τ, R and Sc.
- Growing values of Gr, Gc, K, Ec, τ, and Sc, heat transference rate improves although it declines when magnetic parameter M increases.

Through our study, we have been able to improve our knowledge of fluid dynamics with several facets, therefore throwing light on issues that have not been thoroughly recorded in the existing literature. In addition to that, this study establishes a solid framework for future studies, which opens up potential for research and innovation. This model is compatible with nanofluids, hybrid nanofluids, and tri-hybrid nanofluids, all of which have distinct fluid properties.

Author Contributions

All authors examined and corrected the whole manuscript. Throughout the writing process, all authors have read and approved the final version of the manuscript.

Acknowledgments

Conflict of Interest

The authors declared no potential conflicts of interest concerning the research, authorship, and publication of this article.

Funding

Data Availability Statements

The datasets generated and/or analyzed during the current study are available from the corresponding author on reasonable request.

Nomenclature

u	Horizontal velocity component [m/s]	T_{ref}	A reference temperature
v	Vertical velocity component [m/s]	k	The thermophoretic coefficient
x	Horizontal Cartesian coordinates [m]	λ_g and λ_p	The thermal conductivities of the fluid and diffused particles, respectively
y	Vertical Cartesian coordinates [m]	K_n	The Knudsen numbers
B_0	The magnetic induction	τ	Thermoporesis parameter
T_w	The wall temperature of the inclined plate	M	The magnetic field parameter
T_∞	The ambient temperature	G	The micro-rotation parameter
ν	The kinematic viscosity	Gr	The local thermal Grashof number
g	The gravity	Gc	The local solute Grashof number
(β_T, β_C)	The coefficient of thermal and volumetric expansions	K	The coupling parameter
T	The temperature of boundary layer fluid	Pr	The Prandtl number
C	The concentration of boundary layer fluid	R	The thermal radiation parameter
C_∞	The ambient concentration	Ec	The Eckert number
σ	The electrical conductivity	Sc	The Schmidt number
λ	The fluid thermal conductivity	Q	Heat absorption parameter
ρ	The fluid density	f_w	Wall mass transfer dimension less coefficient
C_p	Specific heat	Cf	The skin friction coefficient
q_r	Radiative heat flux	Cm	The couple stress coefficient
Q_0	Heat absorption/generation coefficient	$q_w(x)$	Heat transfer rate

μ	The dynamic viscosity	Sh_x	Mass transfer rate
D	Molecular diffusivity	Re_x	Reynolds number
V_T	The thermophoretic velocity	q_r	Heat flux radiation
U_0	The uniform plate velocity	η	Similarity variable
$v_w(x)$	The fluid mass injection or suction	N	Angular Velocity
σ_*	The Stefan-Boltzmann constant	θ	Dimensionless temperature
k_*	The mean absorption coefficient		

References

[1] Eringen, A.C., Theory of micropolar fluids, *Journal of Mathematics and Mechanics*, 16(1), 1966, 1–18.

[2] Eringen, A.C., Theory of Thermomicrofluids, *Journal of Mathematical Analysis and Applications*, 38, 1972, 480-496.

[3] Kumar, K.A., Sugunamma, V., Sandeep, N., Mustafa, M., Simultaneous solutions for first order and second order slips on micropolar fluid flow across a convective surface in the presence of Lorentz force and variable heat source/sink, *Scientific Reports*, 9(1), 2019, 14706.

[4] Anantha Kumar, K., Sugunamma, V., Sandeep, N., Influence of viscous dissipation on MHD flow of micropolar fluid over a slendering stretching surface with modified heat flux model, *Journal of Thermal Analysis and Calorimetry*, 139, 2020, 3661-3674.

[5] Chiu, C.P., Chou, H.M., Free convection in the boundary layer flow of a micropolar fluid along a vertical wavy surface, *Acta Mechanica*, 101, 1993, 161–174.

[6] Hassanien, I.A., Gorla, R.S.R., Heat transfer to a micropolar fluid from a non-isothermal strething sheet with suction and blowing, *Acta Mechanica*, 84, 1990, 191–199.

[7] Gorla, R.S.R., Mixed convection boundary layer flow of a micropolar fluid on a horizontal plate, *Acta Mechanica*, 108, 1995, 101–109.

[8] Sharma, R.P., Shaw, S., MHD non-Newtonian fluid flow past a stretching sheet under the influence of non-linear radiation and viscous dissipation, *Journal of Applied and Computational Mechanics*, 8(3), 2022, 949-961.

[9] Dash, A.K., Mishra, S.R., Free convection of micropolar fluid over an infinite inclined moving porous plate, *Journal of Applied and Computational Mechanics*, 8(4), 2022, 1154-1162.

[10] Ibrahim, S.M., Reddy, T.S., Reddy, N.B., Radiation and mass transfer effects on MHD free convective stream of micropolar fluid past a stretching surface embedded in a non-Darcian porous medium with heat generation, *International Scholarly Research Notices*, 2013, 2013, 1534750.

[11] Roja, P., Reddy, T., Ibrahim, S.M., Lorenzini, G., Che Sidik, N.A., The Effect of thermophoresis on MHD stream of a micropolar liquid through a porous medium with variable heat and mass flux and thermal radiation, *CFD Letters*, 14(5), 2022, 106-124.

[12] Harish, M., Ibrahim, S.M., Kumar, P.V., Lorenzini, G., A Study on Effects of Thermal Radiative Dissipative MHD Non-Newtonian Nanofluid above an Elongating Sheet in Porous Medium, *Journal of Applied and Computational Mechanics*, 9(4), 2023, 945-954.

[13] Krishna, M.V., Anand, P.V.S., Chamkha, A.J., Heat and mass transfer on free convective flow of amicropolar fluid through a porous surface with inclined magnetic field and hall effects, *Special Topics & Reviews in Porous Media: An International Journal*, 10(3), 2019, 1-10.

[14] Abbas, N., Nadeem, S., Khan, M.N., Numerical analysis of unsteady magnetized micropolar fluid flow over a curved surface, *Journal of Thermal Analysis and Calorimetry*, 147(11), 2022, 6449-6459.

[15] El-Arabawy, H.A., Effect of suction/injection on the flow of a micropolar fluid past a continuously moving plate in the presence of radiation, *International Journal of Heat and Mass Transfer*, 46(8), 2003, 1471-1477.

[16] Hossain, M.A., Alim, M.A., Natural convection-radiation interaction on boundary layer flow along a thin vertical cylinder, *Journal of Heat and Mass Transfer*, 32, 1997, 515-520.

[17] Hossain, M.A., Takhar, H.S., Thermal radiation effects on natural convection flow over an isothermal horizontal plate, *Heat and Mass Transfer*, 35, 1999, 321-326.

[18] Abd El-Naby, M.A., Elsayed, M.E.E., Nader, Y.A., Finite difference solution of radiation effects on MHD unsteady free convection flow over vertical plate with variable surface temperature, *Journal of Applied Mathematics*, 21(1), 2003, 65-86.

[19] Hossain, M.A., Viscous and Joule heating effects on MHD free convection flow with variable surface temperature, *International Journal of Heat and Mass Transfer*, 1992, 35, 3485-3487.

[20] Mamun, A.A., Chowdhury, Z.R., Azim, M.A., Molla, M.M., MHD-conjugate heat transfer analysis for a vertical flat plate in presence of viscous dissipation and heat generation, *International Journal Communications in Heat and Mass Transfer*, 35, 2008, 1275-1280.

[21] Palani, G., Kwang, Y.K., Joule heating and viscous dissipation effects on MHD flow past a semi-infinite inclined plate with variable surface temperature, *Journal of Engineering Thermophysics*, 20, 2011, 501-517.

[22] Rashad, A.M., Abbasbandy, S., Chamkha, A.J., Mixed convection flow of a micropolar fluid over a continuously moving vertical surface immersed in a thermally and solutally stratified medium with chemical reaction, *Journal of the Taiwan Institute of Chemical Engineers*, 45(5), 2014, 2163-2169.

[23] Eid, M.R., Jamshed, W., Goud, B.S., Ibrahim, R.W., El Din, S.M., Abd-Elmonem, A., Abdalla, N.S.E., Mathematical analysis for energy transfer of micropolar magnetic viscous nanofluid flow on permeable inclined surface and Dufour impact, *Case Studies in Thermal Engineering*, 49, 2023, 103296.

[24] Rafique, K., Alotaibi, H., Nofal, T.A., Anwar, M.I., Misiran, M., Khan, I., Numerical solutions of micropolar nanofluid over an inclined surface using Keller box analysis, *Journal of Mathematics*, 2020, 2020, 1-13.

[25] Goren, S.L., Thermophoresis of aerosol particles in laminar boundary layer on flat plate, *Journal of Colloid and Interface Science*, 61(1), 1977, 77–85.

[26] Goldsmith, P., May, F.G., *Diffusiophoresis and Thermophoresis in Water Vapour Systems: Aerosol Science*, Academic Press, London, UK, 1966.

[27] Abbas, A., Ashraf, M., Chamkha, A.J., Combined effects of thermal radiation and thermophoretic motion on mixed convection boundary layer flow, *Alexandria Engineering Journal*, 60(3), 2021, 3243-3252.

[28] Das, K., Jana, S., Kundu, P.K., Thermophoretic MHD slip flow over a permeable surface with variable fluid properties, *Alexandria Engineering Journal*, 54(1), 2015, 35-44.

[29] Swain, K., Mahanthesh, B., Mebarek-Oudina, F., Heat transport and stagnation-point flow of magnetized nanoliquid with variable thermal conductivity, Brownian moment, and thermophoresis aspects, *Heat Transfer*, 50(1), 2021, 754-767.

[30] Hazarika, S., Ahmed, S., Impact of thermal conductivity on a horizontal absorbent isothermal wall in a porous medium with heat source and thermophoretic forces: Application of suction/blowing, *Heat Transfer*, 51(8), 2022, 7972-7989.

[31] Nabwey, H.A., Rashad, A.M., Mahdy, A.E.N., Shaaban, S.M., Thermal conductivity and thermophoretic impacts of micropolar fluid flow by a horizontal absorbent isothermal porous wall with heat source/sink, *Mathematics*, 10(9), 2022, 1514.

[32] Irfan, M., Farooq, M.A., Thermophoretic MHD free stream flow with variable internal heat generation/absorption and variable liquid characteristics in a permeable medium over a radiative exponentially stretching sheet, *Journal of Materials Research and Technology*, 9(3), 2020, 4855-4866.

[33] Yu, Y., Madhukesh, J.K., Khan, U., Zaib, A., Abdel-Aty, A.H., Yahia, I.S., Alqahtani, M.S., Wang, F., Galal, A.M., Nanoparticle aggregation and thermophoretic particle deposition process in the flow of micropolar nanofluid over a stretching sheet, *Nanomaterials*, 12(6), 2022, 977.

[34] Pakravan, H.A., Yaghoubi, M., Combined thermophoresis, Brownian motion and Dufour effects on natural convection of nanofluids, *International Journal of Thermal Sciences*, 50(3), 2011, 394-402.

[35] Bahiraei, M., Hosseinalipour, S.M., Particle migration in nanofluids considering thermophoresis and its effect on convective heat transfer, *Thermochimica Acta*, 574, 2013, 47-54.

[36] Anbuchezhian, N., Srinivasan, K., Chandrasekaran, K., Kandasamy, R., Thermophoresis and Brownian motion effects on boundary layer flow of nanofluid in presence of thermal stratification due to solar energy, *Applied Mathematics and Mechanics*, 33, 2012, 765-780.

[37] Batchelor, G.K., Shen, C., Thermophoretic deposition of particles in gas flowing over cold surfaces, *Journal of Colloid and Interface Science*, 107(1), 1985, 21-37.

[38] Talbot, L., Cheng, R.K., Schefer, A.W., Wills, D.R., Thermophoresis of particles in a heated boundary layer, *Journal of Fluid Mechanics*, 101, 1980, 737-758.

[39] Mills, A.F., Hang, X., Ayazi, F., The effect of wall suction and thermophoresis on aerosol-particle deposition from a laminar boundary layer on a flat plate, *International Journal of Heat and Mass Transfer*, 27, 1984, 1110–1114.

[40] Jalili, B., Ganji, A.M., Shateri, A., Jalili, P., Ganji, D.D., Thermal analysis of non-Newtonian visco-inelastic fluid MHD flow between rotating disks, *Case Studies in Thermal Engineering*, 49, 2023, 1-17.

[41] Jalili, P., Azar, A.A., Jalili, B., Ganji, D.D., The HAN method for a thermal analysis of forced non-Newtonian MHD Reiner-Rivlin viscoelastic fluid motion between two disks, *Heliyon*, 9(6), 2023, 1-18.

[42] Jalili, P., Azar, A.A., Jalili, B., Ganji, D.D., Study of nonlinear radiative heat transfer with magnetic field for non-Newtonian Casson fluid flow in a porous medium, *Results in Physics*, 48, 2023, 1-27.

[43] Dogonchi, A.S., Bondareva, N.S., Sheremet, M.A., El-Sapa, S., Chamkha, A.J., Shah, N.A., Entropy generation and heat transfer performance analysis of a non-Newtonian NEPCM in an inclined chamber with complicated heater inside, *Journal of Energy Storage*, 72, 2023, 108745.

[44] Dogonchi, A.S., Karimi, N., Hu, G.J., Chamkha, A.J., Elmasry, Y., Thermo-economic and entropy generation analyses of magnetic natural convective flow in a nanofluid-filled annular enclosure fitted with fins, *Sustainable Energy Technologies and Assessments*, 46, 2021, 101274.

[45] Dogonchi, A.S., Waqas, M., Afshar, S.R., Seyyedi, S.M., Hashemi-Tilehnoee, M., Chamkha, A.J., Ganji, D.D., Investigation of magneto-hydrodynamic fluid squeezed between two parallel disks by considering Joule heating, thermal radiation, and adding different nanoparticles, *International Journal of Numerical Methods for Heat & Fluid Flow*, 30(2), 2020, 659-680.

[46] Mondal, H., Unsteady MHD micropolar fluid in a stretching sheet over an inclined plate with the effect of non-linear thermal radiation and Soret-Dufour, *Journal of Thermal Engineering*, 5(6), 2019, 205-213.

[47] Brewster, M.Q., *Thermal radiative Transfer and properties*, John Wiley and Sons, New York, 1992.

ORCID ID

Shaik Mohammed Ibrahim https://orcid.org/0000-0002-7918-5364

Gurram Dharmaiah https://orcid.org/0000-0001-7788-5773

Giulio Lorenzini https://orcid.org/0000-0002-5676-8575

Publisher's Note Shahid Chamran University of Ahvaz remains neutral with regard to jurisdictional claims in published maps and institutional affiliations.